Dalton Transactions

Accepted Manuscript

ROYAL SOCIETY OF CHEMISTRY

www.rsc.org/dalton

Graphic Image:

Novel ultrasonication assistant method was developed to synthesize monodisperse Fe_3O_4@SiO_2-Ag nanospheres which exhibited excellent antibacterial activities against both *Staphylococcus aureus* and *Escherichia coli*.

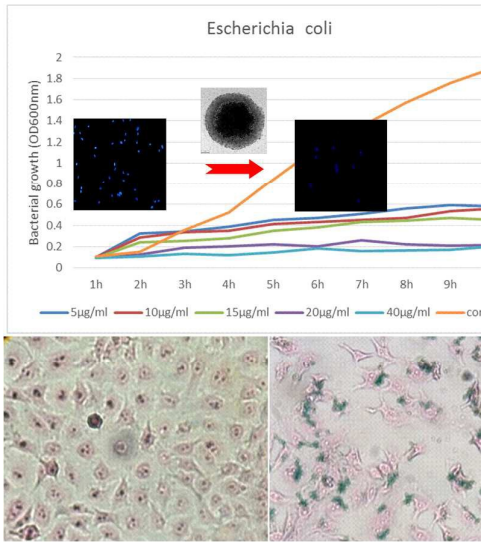

Facile Ultrasonic Assistant Method for Fe_3O_4@SiO_2-Ag Nanospheres with Excellent Antibacterial Activity

Shuang-Sheng Chen[1]†,Hui Xu[1]†,Hua-Jian Xu[2], Guang-Jin Yu[1], Xing-Long Gong[4], Qun-Ling Fang[2]*, Ken Cham-Fai Leung[3], Shou-Hu Xuan[4], Qi-Ru Xiong[1]**

[1] *Department of Chirurgery, Affiliated Hospital 1, Anhui Medical University, Hefei 230032, P.R. China*

[2] *School of Medical Engineering, Hefei University of Technology, Hefei, 230009, P.R. China*

[3] *Department of Chemistry and Partner State Key Laboratory of Environment and Biological Analysis, Hong Kong Baptist University, Kowloon, Hong Kong SAR, P. R. China*

[4] *CAS Key Laboratory of Mechanical Behavior and Design of Materials, Department of Modern Mechanics, University of Science and Technology of China, Hefei, 230026, P. R. China*

Corresponding authors:

Qi-Ru Xiong
E-mail: xiongqiru2012@126.com

Guang-Jin Yu
E-mail: yugj7806290@sohu.com

Qun-Ling Fang
E-mail: fql.good@hfut.edu.cn

† These authors contributed equally to this work.

Abstract:
To increase the monodispersity of the magnetic hybrid nanocomposites, novel ultrasonic method was introduced to synthesize uniform Fe_3O_4@SiO_2-Ag nanospheres. The immobilized Ag nanocrystals were tunable by varying the experimental condition. The antibacterial assay indicated that the Fe_3O_4@SiO_2-Ag nanospheres exhibited excellent antibacterial activities against the *Staphylococcus aureus* and *Escherichia coli*, in which the minimum inhibition concentrations (MIC) were 40 μg/mL and 20 μg/mL, respectively. The live/dead bacterial cell fluorescence stain assay agreed well with the antibacterial assay. The CCK-8 results indicated these nanospheres were bio-compatible for human normal cells, while presented a relative cytotoxicity against the HepG2 tumor cells. These nanospheres could be easily uptake by the cells and they could affect the bacterial cells both inside and outside the cell membrane, which enable them be promisingly applied in future biomedical areas.

Keywords: Ultrasonication; Core/shell; Ag; Antibacterial; Cell uptake

1. Introduction

Pathogenic bacteria have greatly threatened public health since they bring about terrible infectious diseases. To meet with the increasing demands for hygiene in public health care, various efforts have been done to develop highly effective antibacterial agents [1-4]. In recent years, with the rapid development of nanotechnology, more and more research in this area has been focused on the nano-antibacterial [5-8]. Silver has been used as antibacterial agents for centuries to deal with infections, burns and chronic wounds due to its low toxicity to human body [9-14]. It was found that by decreasing the size of the Ag particles, their antibacterial activities intensively enhanced. Therefore, the investigation of the Ag based nano-antibacterial agent would be much helpful for its future commercial production and application in the clothing, food packaging and bandages [15-16].

Though the principle was not very clear, the most acceptable antibacterial mechanism of Ag nanoparticles was believed to be the release of Ag ions, which can combine the –SH groups and lead to the inactivation of the proteins[17-19]. Besides the size and shape, the stability of the nanoparticles also exhibited high influence on the antibacterial activity [10,20]. Therefore, the Ag nanoparticles were immobilized onto various substrates such as silica, polymer, iron oxide, carbon, layered double hydroxide (LDH), zeolite, etc [21-30]. This method not only prevented the aggregation of the Ag nanoparticles but also enhanced their antibacterial capacity. Present research demonstrated that the Ag based nano-antibacterial agents could affect the bacteria both inside and outside the cell membrane by catalyzing the complete

destructive oxidation of the microorganisms [18,31]. To this end, uniform Ag based nanocomposites with small sizes are desirable for high performance nano-antibacterial agents.

Environmental friendly methods were favorable for the preparation of nano-antibacterial agents since they can reduce biological hazard for living cells [18,32-36]. Recently, several *in situ* fabrication strategies were developed so that the residue of the toxic reducing agents (such as KBH_4 and hydrazine) could be eliminated in the final system. By utilizing the reducing characteristic of polydopamine (PDA), Ag nanoparticles with different size and coverage were coated onto the surface of PS/PDA microspheres and the thereof antibacterial agent exhibited enhanced performance against the *Escherichia coli* and *Staphylococcus aureus* [37]. Similarly, the Ag nanoparticles could be directly immobilized on the LDH film by simply immersing the film into the $AgNO_3$ aqueous solution due to the self-redox reaction [28]. This method offered a good opportunity for their practical application in antimicrobial surfaces.

Moreover, some risks of using Ag based nano-antibacterial agent were also presented because the high concentration of residual nanosilver in solution was toxic. The potential strategy for solving this problem would be the combination of magnetic characteristic with the antibacterial property, so that the antibacterial agent could be targeting richen in certain area or magnetically separated from the working area after the bacteria have been killed. During the past decade, several magnetic antibacterial agents such as $Ag@Fe_3O_4$ core shell nanoparticles/nanospheres, $Fe_3O_4@SiO_2@Ag$

sub-microspheres/janus nanorods, and Ag-Fe_2O_3 heteromer were developed [23, 38-42]. Although these materials exhibited high antibacterial performance, the detailed nanostructure dependent antibacterial activity was unknown and mechanism of their action was not very clear. In consideration of the green preparation and easy conduction, novel method for multifunctional antibacterial agent is still needed.

In this work, a facile ultrasonic assistant method was reported for easily and environmental friendly synthesizing of Fe_3O_4@SiO_2-Ag nanospheres. This method presented three unique characteristics: (1) Different from the previously reported large Fe_3O_4@SiO_2-Ag particles, the average size of the obtained product was about 200 nm. They were uniform and could be well dispersed within the PBS to form stable suspension. (2) The small Ag nanoparticles were synthesized under the help of sonication and neither reductant nor toxic reagents were used in this procedure. Moreover, the size of the Ag nanoparticles could be controlled by varying the reaction time. (3) The as prepared nanoparticles can be used as antibacterial agents against *Escherichia coli* and *Staphylococcus aureus*. Due to the small size, these materials also could be uptake by cells which would be much helpful for further investigating their antibacterial mechanisms.

2. Results and Discussion

2.1 Preparation and characterization of Fe_3O_4@SiO_2-Ag nanospheres.

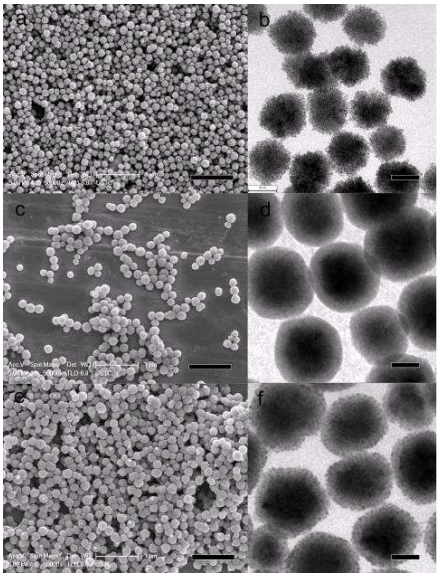

Figure 1. SEM and TEM images of the as prepared Fe_3O_4 (a,b), Fe_3O_4@SiO_2-NH_2 (c,d), and Fe_3O_4@SiO_2-Ag nanospheres. The scale bars for SEM and TEM image are 1μm and 90 nm, respectively.

The Fe_3O_4 nanospheres were prepared according to the previously reported solvothermal method [43]. The SEM images confirmed that the as-obtained product were uniform with an average diameter of 150 nm. The Fe_3O_4 nanospheres presented a cluster-like nanostructure and they were composed of Fe_3O_4 nanocrystals. The TEM image of the Fe_3O_4 nanosphere clearly approved the above description and the measured size agreed well with the SEM analysis. These Fe_3O_4 nanospheres possessed a rough surface, in which polyacrylic acid polymer was entangled to give large amount of hydrophilic functional groups. Therefore, they can be well suspended within the water or ethanol solution.

The ultra-sonication was applied to synthesize monodispersed Fe_3O_4@SiO_2-NH_2 nanospheres. Firstly, the SiO_2 layer was uniformly coated onto the surface of the Fe_3O_4 nanosphere to form a well defined core shell nanostructure. Due to the preparation was conducted under sonication, the as-formed Fe_3O_4@SiO_2 nanospheres

were monodispersed without large aggregation. At the end of the coating process, APTES was introduced into the synthetic system, thus the surface of the Fe_3O_4@SiO_2 nanospheres was *in situ* modified by a layer of $–NH_2$ group. The ultrasonication is critical to this method and many large aggregates were formed in the product while only magnetic or mechanic stirring was conducted. The SEM image show in Figure 1c demonstrated the well dispersity of the nanospheres synthesized under sonication. Because of the uniform coating, the average size of the Fe_3O_4@SiO_2-NH_2 was larger than the pristine Fe_3O_4 nanospheres. The TEM image shown in Figure 1b further proved the formation of the core shell nanostructure. By calculating 100 particles, the average shell thickness of the SiO_2 layer was about 30 nm. Here, the average shell thickness could be controlled by varying the experimental parameters, such as the concentration of the Fe_3O_4 nanospheres and TEOS.

The preparation of Fe_3O_4@SiO_2-Ag nanospheres was also conducted under the help of ultra-sonication by using the Fe_3O_4@SiO_2-NH_2 as the template. In this process, the -NH_2 group served as a bridge between SiO_2 coating and Ag nanoparticles. Without these functional groups, only a few Ag nanoparticles were decorated on the Fe_3O_4@SiO_2 nanospheres. After the $[Ag(NH_3)_2]^+$ ions were introduced into the Fe_3O_4@SiO_2-NH_2 suspension, they would be slowly reduced by the -NH_2 group and ethanol solvent to give the Ag particles. Figure 1e showed the SEM image of the Fe_3O_4@SiO_2-Ag nanospheres which clearly indicated that the as-prepared product presented monodispersibility without large aggregation. The average size of the product was similar to the Fe_3O_4@SiO_2-NH_2 nanospheres. However, from TEM

image (Figure 1f), it was found that the surface of the Fe_3O_4@SiO_2-Ag nanospheres was much rougher than the Fe_3O_4@SiO_2-NH_2. All the surface of the nanospheres were decorated with small dots with size about 3-5 nm and the coverage ratio was very high. Here, sonication was important for such a high loading. During the preparation, the sonication accelerated the reducing process since "hot points" with high pressure, temperature, and reductive circumstance were formed in the solution [44,45]. Therefore, the Ag nanoparticles can directly cover on the surface of the template with a high coverage ratio in this method.

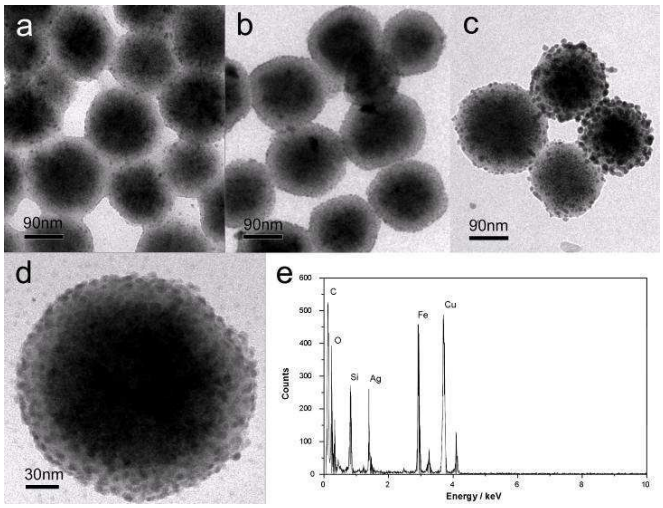

Figure 2. TEM images of the Fe_3O_4@SiO_2-Ag nanospheres prepared under different ultrasonic time: a) 1 h; b) 3 h; c) 10 h. d) and e) are the large magnification TEM image and EDS spectra for the nanospheres prepared under 3h.

Here, the sonication time showed high influence on the Ag coverage on the Fe_3O_4@SiO_2 nanospheres. Figure 2a presents the TEM image of the Fe_3O_4@SiO_2-Ag nanospheres under 1h sonication. Though the Ag nanoparticles were successfully immobilized on the Fe_3O_4@SiO_2 nanospheres, the coverage in this case was not very high. As soon as the time prolonged to be 3 h, the uniform coating of Ag layer was obtained. The further increasing of the reaction time is not good for the preparation of

the Fe_3O_4@SiO_2-Ag nanospheres. It was fount that the size of the Ag nanoparticles critically increased from 3-5 nm to 10-20 nm. Moreover, some Ag-Ag nanoparticles aggregations were found on the nanospheres' surface. Therefore, 3h is the optimum time for this preparation. The typical high magnification TEM image of a single Fe_3O_4@SiO_2-Ag nanosphere (Figure 2d) indicated that the Ag nanodots homogeneously distributed on the surface. These Ag nanodots were tightly anchored on the Fe_3O_4@SiO_2 core with the help of abundant amine groups. The EDS result in Figure 2e also indicated that this nanosphere was composed of Fe, Si, O, and Ag element, which further hinted the successful preparation.

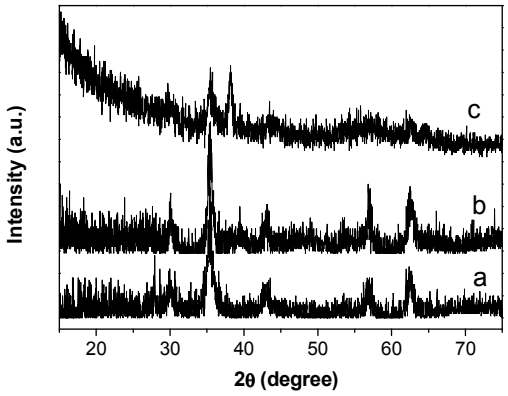

Figure 3. XRD diffraction patterns of the as-prepared Fe_3O_4 (a), Fe_3O_4@SiO_2-NH_2 (b), and Fe_3O_4@SiO_2-Ag (c) nanospheres.

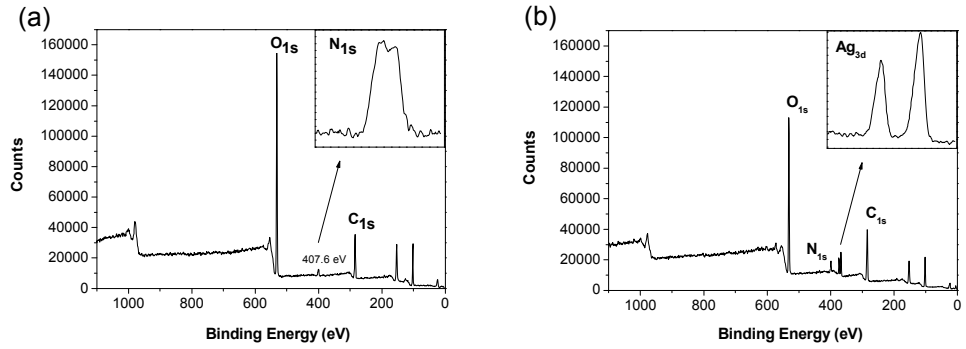

Figure 4. XPS spectrums of the as-prepared Fe_3O_4@SiO_2-NH_2 (a) and Fe_3O_4@SiO_2-Ag nanospheres (b); The insert for (a) and (b) are the N1s and Ag3d spectrums, respectively.

The XRD spectra of the as-prepared samples at different steps were indicated in Figure 3, including the Fe_3O_4, Fe_3O_4@SiO_2-NH_2, and Fe_3O_4@SiO_2-Ag nanospheres. The broad nature of the diffraction peaks for Fe_3O_4 illustrated the cluster-like nanostructure. Because of the amorphous crystallinity of the SiO_2 shell, novel obvious peak for the SiO_2 has not been observed in the Fe_3O_4@SiO_2-NH_2 product. The further immobilization of Ag nanoparticles on the Fe_3O_4 nanospheres lead to the presence of a novel broad diffraction peaks located at 38°. According to the Scherrer formula, the average size of the Ag nanoparticles was calculated to be 5 nm [46]. This result also agreed well with the above TEM and SEM analysis. XPS was also used for analyze the surface state of the materials. As shown in Figure 4a, C1s, O1s, Si2p, N1s signal peaks are distinct in the XPS spectra, which demonstrated the Fe_3O_4 nanospheres were well encapsulated by the SiO_2 shell. The relative weak peak for N1s indicated the SiO_2 shell was functionalized by amine group. After the Ag nanoparticles were decorated on the Fe_3O_4@SiO_2 nanospheres, the strong peaks at a binding energy of about 368 and 374 eV were presented which demonstrated the metallic Ag with zero covalent state were formatted in the nanospheres [37].

2.2 Antibacterial properties of Fe_3O_4@SiO_2-Ag nanospheres.

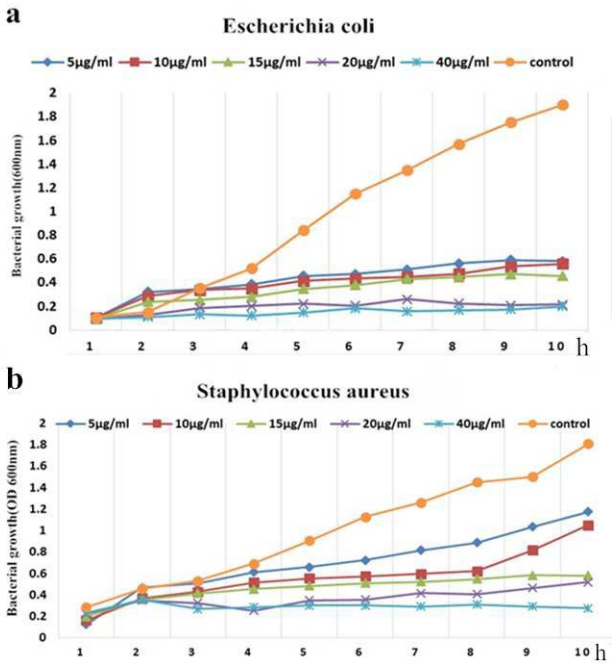

Figure 5. Bacterial growth curves in LB media with Fe_3O_4@SiO_2-Ag nanospheres. Different concentrations of the nanospheres were used in cultures of *Escherichia coli* (a) and *Staphylococcus aureus* (b).

Because of its low toxicity to humans, both silver and silver based nanomaterials were extensively used as antimicrobial agents due to their strong inhibitory effects for a wide range of bacteria [10,47]. In this work, both *Escherichia coli* and *Staphylococcus aureus* were applied as the bacterium models to study the antibacterial properties of the Fe_3O_4@SiO_2-Ag nanospheres.

Here, a modified Kirby-Bauer method was used to quantitatively investigate the antibacterial activities of the Fe_3O_4@SiO_2-Ag nanospheres. The Fe_3O_4@SiO_2-Ag nanospheres which were prepared in the optimum condition (3h) were chosen as a typical agent to plot the bacterial inhibition growth curves. Figure 5 shows the antibacterial effect of Fe_3O_4@SiO_2-Ag nanospheres against *Escherichia coli* and *Staphylococcus aureus* after culturing from 1 to 10 h. In comparison to the blank control groups, the growth rates of the *Escherichia coli* were clearly inhibited by

using these nano-antibacterial agents (Figure 5a). Even under a low concentration of nano-antibacterial agents (5 μg/mL), the bacterial was critically retarded. In this process, the higher the concentration, the better the antibacterial effects. Observably, the minimum inhibition concentrations (MIC) the Fe_3O_4@SiO_2-Ag nanospheres was just 20 μg/mL, which was smaller than the previously reported Ag-SiO_2, Ag-Fe_3O_4, and Ag-TiO_2 [48-50]. Similarly, this nano-antibacterial agent also exhibited effective antibacterial activities to the *Staphylococcus aureus* and the MIC for *Staphylococcus aureus* was estimated to be 40 μg/mL (Figure 5b). The *Staphylococcus aureus* and *Escherichia coli* were belonged to Gram-positive and Gram-negative bacteria respectively. It was reported that the membrane of the Gram-positive bacteria was thicker than the Gram-negative bacteria, thus the former was more stable than the later [51]. To this end, it was reasonable to find out that the *Escherichia coli* was more sensitive to Fe_3O_4@SiO_2-Ag nanospheres than the *Staphylococcus aureus*, which also agreed well with the previous work.

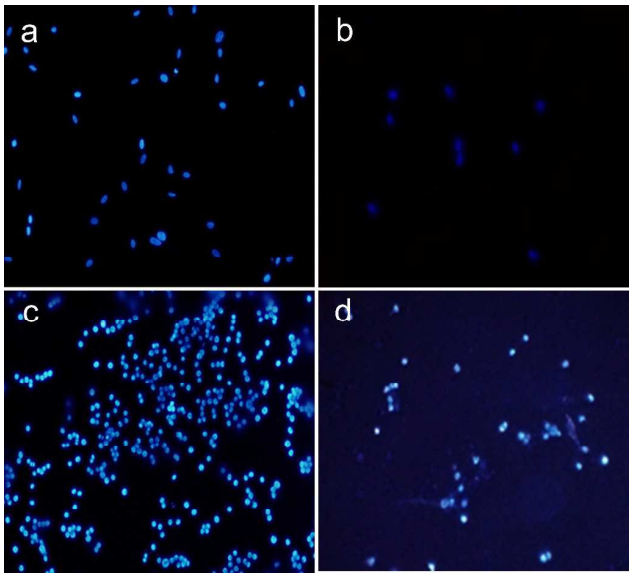

Figure 6. Fluoresecnt images of the antibacterial activities of the Fe_3O_4@SiO_2-Ag nanospheres against *Escherichia coli* (a,b) and *Staphylococcus aureus* (c,d).

To further investigate the antibacterial activities of the Fe_3O_4@SiO_2-Ag nanospheres, live/dead bacterial cell fluorescence stain assay was used to study the state of the bacterial cell before and after treated with the anti-bacterial agents. In this work, after the bacterial cells were incubated with Fe_3O_4@SiO_2-Ag nanospheres for 12 h, blue fluorescent dye was employed to stain the live cells. Figure 6a shows the fluorescent image of the *Escherichia coli* without treating with the nano-antibacterial agent. The strong blue fluorescence point in the image clearly indicated the living of the bacterial cells. However, after the incubation, almost no fluorescence was observed (Figure 6b). These results clearly indicated that the *Escherichia coli* were major inhibited in the presence of the nano-antibacterial agent. Moreover, similar results were also obtained for the *Staphylococcus aureus* (Figure 6c,d), which further demonstrated that the as-prepared Fe_3O_4@SiO_2-Ag nanospheres showed unique effective antibacterial activities and these analysis agreed well with the observation

from antibacterial assays.

2.3 Cytotoxicity and uptake of Fe_3O_4@SiO_2-Ag nanospheres to cancer cell.

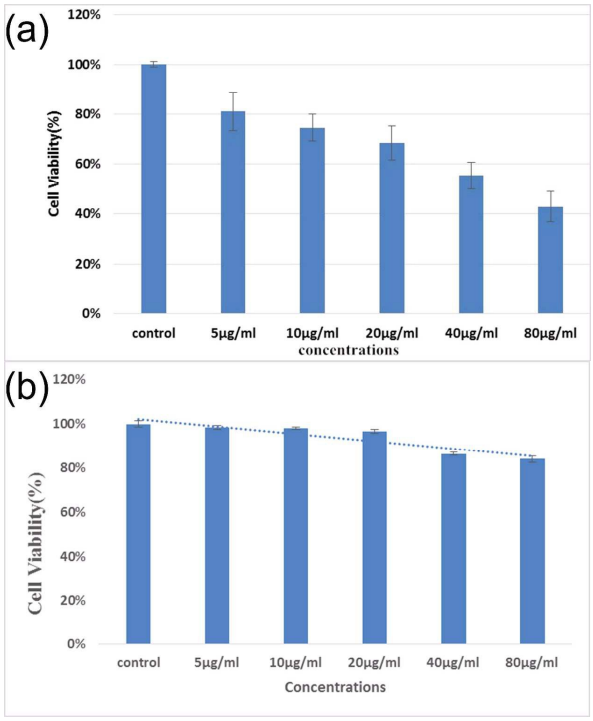

Figure 7. In vitro cytotoxicity of Fe_3O_4@SiO_2-Ag nanospheres against HepG2 cells (a) and HUVEC cells (b) after incubation at 37℃ for 24 h.

The Fe_3O_4@SiO_2-Ag nanospheres also exhibited relative cytotoxicity to cancer cells. Hepatocellular carcinoma is the fifth most-common cancer in the world. The HepG2 is a perpetual cell line consisting of human liver carcinoma cells, thus they were chosen for testing the *in vitro* cytotoxicity of the as-prepared Fe_3O_4@SiO_2-Ag nanospheres. Firstly, the HepG2 cells were incubated with these nanospheres at 37 ℃ for 24 h. Then the in vitro cytotoxicity was measured using the Cell Counting Kit-8(CCK-8) assay. Here, the influence of the Fe_3O_4@SiO_2-Ag nanospheres concentration was also investigated and they were ranged from 0-80 μg/mL (Figure 7a). It was found that the Fe_3O_4@SiO_2-Ag nanospheres showed unique effect on

cytotoxicity against the HepG2 cells. Only 80% cells were viable when a low concentration of these nanospheres (5 μg/mL) was introduced into the system. With further increasing of the nanospheres, the cell viability decreased and it reduced to 44% when the concentration reaches to 80 μg/mL. Based on the above analysis, it could be concluded that the Fe_3O_4@SiO_2-Ag nanospheres were toxic to the cancer cells which enable them be potentially applied as treating agents for cancer.

Safety is the main concern in the application of a nano-agent for clinical therapeutics, thus the cytotoxicity of the Fe_3O_4@SiO_2-Ag nanospheres to the normal cells was investigated. In this work, the in vitro biocompatibility of the nanoparticles to the HUVEC cells (Human Umbilical Vein Endothelial Cells) was tested by using the CCK-8 assay. As shown in Figure 7b, the anti-bacterial materials did not present significant cytotoxicity against the HUVEC cells and the cell viability can keep 80% when the concentration of the nanospheres was increased to as high as 80 μg/mL. It indicated that the Fe_3O_4@SiO_2-Ag nanospheres showed good cytocompatibility with human normal cells.

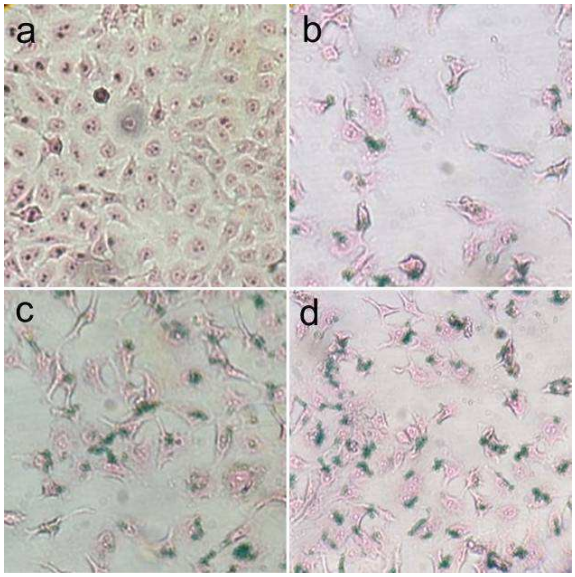

Figure 8. Cellular uptake of Fe_3O_4@SiO_2-Ag nanospheres a) 0, b) 10, c) 20, and d) 40 μg/mL in HT29 cells evaluated by Prussian blue staining.

The cellular uptake was studied to further investigated action mechanism of the Fe_3O_4@SiO_2-Ag nanospheres to cancer cells. Here, Prussian blue staining was employed to evaluate the cellular uptake of Fe_3O_4@SiO_2-Ag nanospheres in HepG-2 cells. Firstly, the HepG-2 cells were incubated with different concentrations of Fe_3O_4@SiO_2-Ag nanospheres for 20 h. Then, they were fixed for 30 min by using 4% paraformaldehyde. After treating them with Perls' reagent, the results were finally obtained by using a light microscopy. As shown in Figure 8 were the images of the prussian blue staining cells with and without incubation of the Fe_3O_4@SiO_2-Ag nanospheres. Because of the monodispersity characteristic, these small Fe_3O_4@SiO_2-Ag nanospheres could insert into the cells very easily. Figure 8b showed the image obtained by treating the cells with 10 μg/mL nanospheres. In comparison to the blank experiment, blue areas were clearly observed which indicated the Fe_3O_4@SiO_2-Ag nanospheres were successfully uptake by the HepG-2. With

increasing of the concentration, the uptake ratio increased (Figure 8c,d). To this end, the high cellular uptake must be another reason for their excellent cytotoxicity. Moreover, these Fe_3O_4@SiO_2-Ag nanospheres were magnetic and they could be richen in the disease area under applying a magnetic field. Since these nanospheres were bio-compatible to human normal cells, they could be used as the magnetic targeting therapeutic nano-agent to cancer cells without any terribly by-damage to the normal cells. To this end, the further investigation of these composite nanoparticles in cancer treatment was attractive.

2.4 Antibacterial mechanism of Fe_3O_4@SiO_2-Ag nanospheres.

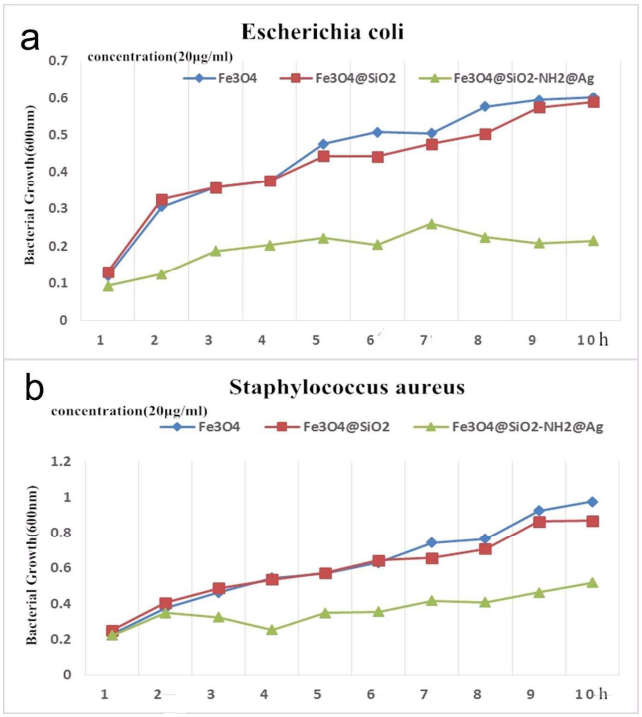

Figure 9. Bacterial growth curves in LB media with Fe_3O_4, Fe_3O_4@SiO_2 and Fe_3O_4@SiO_2-Ag nanospheres. The concentrations of the nanospheres were kept at 20 μg/mL in cultures of *Escherichia coli* (a) and *Staphylococcus aureus* (b).

To further investigate the anti-bacterial mechanism, the bacterial inhibition growth curves of the Fe_3O_4, Fe_3O_4@SiO_2 and Fe_3O_4@SiO_2-Ag nanospheres were performed. Under the same dosage, Fe_3O_4 and Fe_3O_4@SiO_2 nanospheres showed could not inhibit both strains of the bacterial growth, while the Fe_3O_4@SiO_2-Ag showed the significant inhibition of proliferation to the bacterial cells (Figure 9). This result indicated the anti-bacterial activity of the Fe_3O_4@SiO_2-Ag nanospheres was come from the Ag component immobilized on the surface of the Fe_3O_4@SiO_2 nanospheres.

On the basis of above analysis and the results in the literature, the antibacterial activities of the Fe_3O_4@SiO_2-Ag nanospheres were ascribed to the following reasons: Firstly, the antibacterial activity of the nanospheres was inherited from the Ag nanocrystals. Since these stable Ag nanodots were supported on the surface of the SiO_2 shell, they can exhibit enhanced antibacterial activity by reacting with more sulfur-containing proteins in bacterial cell. Secondly, the Ag ions can release from the nanocrystals and de-activate the microorganism cells. The average size of the Ag nanoparticles was only 3-5 nm in our product, thus the Ag ions might be released quicker than the large Ag nanoparticles. These released Ag ions would further cause the structural change of the cells and lead to them death. Third, because of the small size of the uniform Fe_3O_4@SiO_2-Ag nanospheres, these particles could be uptake by cells very easily. More nanospheres could penetrate the cell membrane and directly kill the bacteria inside the cell membrane. Therefore, these Fe_3O_4@SiO_2-Ag nanospheres presented excellent anti-bacterial activities.

It was reported that the release behavior of the Ag ions from the Ag nanoparticles

was pH dependent and more silver ions would be released in acidic environment in comparison to neutral buffer [36]. Moreover, the previous literature indicated that the pH of tumor cells are slightly acidic than the normal cells [52]. Therefore, more Ag ions would be released from the Ag nanoparticles in the tumor cells than the human normal cells. To this end, the Fe_3O_4@SiO_2-Ag nanospheres exhibited higher cytotoxicity in HepG-2 cells than in HUVEC cells.

3. Experimental Section

3.1 Preparation of Fe_3O_4@SiO_2-Ag nanospheres.

All chemicals were of analytical grade and used without further purification. First, the monodispersed Fe_3O_4 nanospheres which were prepared according to the previously reported method [42] were dispersed in ethanol/H_2O/ammonia solution with volume ratio of 30/3/1 under sonication. After half an hour, a certain amount of tetraethyl orthosilicate (TEOS) in ethanol (0.1/1 v/v) was added into the above system. 20 min later, 3-aminopropyltriethoxysilane (APTES) was dropped into the solution to graph $–NH_2$. After further 30 min reaction under ultrasonic, the obtained Fe_3O_4@SiO_2-NH_2 nanospheres was collected by magnetic sepration, washed with ethanol twice and then dispersed in ethanol. To immobilize Ag nanoparticles onto the Fe_3O_4@SiO_2-NH_2 nanospheres, the $[Ag(NH_3)_2]^+$ was firstly prepared by dissolving $AgNO_3$ in ammonia and then they were added into ethanol suspended with Fe_3O_4@SiO_2-NH_2 nanospheres. Under sonication for 1h, poly(vinylpyrrolidone) (PVP) (0.025 g/mL) was added into the system. The reaction was further conducted

for 3 h and the final products were separated, rinsed by ethanol and water for 3 times. After drying the particles in vacuum oven for 12 h, the Fe_3O_4@SiO_2-Ag nanospheres were obtained.

3.2 Antibacterial assays

For the antibacterial activity assays, two bacterial species, *Escherichia coli* (Gram-negative bacteria) and *Staphylococcus aureus* (Gram-positive bacteria), were used in the experiments. Bacterial suspensions were prepared by taking a single colony from the stock bacterial culture with a loop and inoculating 5 mL of sterile nutrient broth medium, which was then incubated in a shaking incubator (37°C at 200 rpm) for 12 h. Later, 30 mL bacterial suspensions were inoculated in 3 mL of liquid nutrient broth medium supplemented with different concentrations of Fe_3O_4@SiO_2-Ag nanospheres. The suspensions were shaken by a shaker at 200 rpm under 37°C, and their bacterial survivals were determined by measuring the optical density (O.D.) of the nutrient broth in both media at a wavelength of 600 nm. The absorbance was sequentially checked from time 0 to 10 h with an interval of 1 h. To further examine the antibacterial properties, the bacteria were stained with the live/dead Bacterial Viability Kit following the protocol (GENMED). Briefly, 3 μL of the fluorescently dyed mixture was added into each milliliter of the bacterial suspensions. Then, the samples were thoroughly mixed and incubated at room temperature in the dark for 15 minutes. To observe the image with a Fluorescence Microscope, 5 μL of the stained bacterial suspension was added to a slide with a square cover slip. For comparison, the antibacterial assays of the Fe_3O_4, Fe_3O_4@SiO_2,

and Fe_3O_4@SiO_2-Ag nanospheres were performed under the same process while keeping the concentration of the nanospheres in 20 μg/mL.

3.3 Cell culture and In vitro cell viability evaluation

HepG2 cells were purchased from the American Type Culture Collection and were cultured in Dulbecco's modified Eagle's medium(GIBCO,USA) supplemented with 10% fetal bovine serum (GIBCO,USA), 2 mM L-glutamine,100 μg/mL streptomycin and 100 U/mL penicillin. The cells were cultured in a 37 ℃ humidified atmosphere with 5% CO_2. The in vitro cytotoxicity of Fe_3O_4@SiO_2-Ag nanospheres against HepG-2 cells was tested using the Cell Counting Kit-8 assay. Cells were seeded in 96-well plates with a density of 1×10^4 cells per well in 100μL of DMEM supplemented with 10% FBS cultured in a humidified atmosphere of 5% CO_2 at 37 ℃ for 24 h. Then, the HepG-2 cells were incubated in the growth medium containing different concentrations (5, 10, 20, 40 and 80 μg mL^{-1}) of Fe_3O_4@SiO_2-Ag nanospheres in the growth medium for another 24 h. Meanwhile, the wells containing the cell medium only were prepared as for the untreated controls. Then, 10 μL of CCK-8 dye was added to each well and the plates were incubated for another 2 h at 37 ℃. Absorbance was measured using single wavelength spectrophotometry at 450 nm using a microplate reader. The relative cell viability was determined by comparing the absorbance at 450 nm with the control wells that containing the cell culture medium only.

3.4 Cellular Uptake

The cellular uptake of Fe_3O_4@SiO_2-Ag nanospheres was evaluated in HepG-2

cells by Prussian blue staining. HepG-2 cells were seeded in a 96-well plate in DMEM containing 10% FBS. After 12 h incubation, medium was replaced with serum-free DMEM containing different concentrations (0, 10, 20, and 40 μg/mL) of Fe_3O_4@SiO_2-Ag nanospheres and incubated for another 20 h. In Prussian blue staining, cells were fixed for 30 min by using 4% paraformaldehyde. After washing with PBS, the cells were incubated with Perls' reagent (4% potassium ferrocyanide and 6% HCl) for 30 min, and followed by a neutral red counterstain. Then the cells were observed using a light microscopy.

3.5 Characterization

X-ray powder diffraction patterns (XRD) of the products were obtained on a Bruker D8 Advance diffractometer equipped with graphite monochromatized Cu Kα radiation (λ = 1.5406 Å). Transmission electron microscopy (TEM) photographs were taken on a high-resolution transmission electron microscope (HRTEM, Tecnai Model JEOL-2010) at an accelerating voltage of 200 kV. The field emission scanning electron microscopy (FE-SEM) images were taken on a JEOL JSM-6700F SEM. X-ray photoelectron spectra (XPS) were measured on an ESCALAB 250.

4. Conclusions

In summary, we present an environmental friendly method to synthesize monodisperse Fe_3O_4@SiO_2-Ag nanospheres under the help of ultrasonication. No toxic reagent was used in the synthesis and the final Ag nanocrystals were uniformly immobilized onto the periphery of Fe_3O_4@SiO_2-NH_2 nanospheres. The antibacterial

assay indicated that the Fe_3O_4@SiO_2-Ag nanospheres exhibited excellent antibacterial activities against the *Staphylococcus aureus* and *Escherichia coli*, in which the MIC were 40 μg/mL and 20 μg/mL, respectively. Moreover, these nanospheres were demonstrated to be cytotoxic to HepG2 while to be compatible to the human normal cells. Due to the magnetic characteristic, they would be applied for targeting treatment. The average size of these nanospheres were about 200nm, thus they could easily uptake by the HepG2 cells. To this end, this kind of nanospheres presented high antibacterial performance since they could destroy the bacterial cells both outside and inside the cell membrane.

Acknowledgement

We acknowledge financial support from the National Natural Science Foundation of China (Grant Nos. 21205026), HKRGC-GRF (201412), and University Grants Committee of Hong Kong SAR (AoE/P-03/08).

Reference

[1] S.Q. Li and N. P. Shah, *Food Chem.*, 2014, **165**, 262-270.
[2] M. Rai, A. Yadav and A. Gade, *Biotechnol. Adv.*, 2009, **27**, 76-83.
[3] I. Kouidmi, R. C. Levesque and C. Paradis-Bleau, *Molecular Microbiol.*, 2014, **94**, 242-253.
[4] C. Marambio-Jones and E. M. V. Hoek, *J. Nanopart. Res.*, 2010, **12**, 1531-1551.
[5] Q. L. Li, S. Mahendra, D. Y. Lyon, L. Brunet, M. V. Liga, D. Li and P. J. J. Alvarez, *Water Res.*, 2008, **42**, 4591-4602.
[6] O. L. Galkina, A. Sycheva, A. Blagodatskiy, G. Kaptay, V. L. Katanaev, G. A. Seisenbaeva, V. G. Kessler and A. V. Agafonov, *Surf. & Coating Tech.*, 2014, **253**, 171-179.
[7] W. B. Hu, C. Peng, W. J. Luo, M. Lv, X. M. Li, D. Li, Q. Huang and C. H. Fan, *ACS Nano*, 2010, **4**, 4317-4323.
[8] J. Lee, S. Mahendra and P. J. J. Alvarez, *ACS Nano*, 2010, **4**, 3580-3590.
[9] O. Akhavan, M. Abdolahad, Y. Abdi, S and Mohajerzadeh, *J. Mater. Chem.*, 2011, **21**, 387-393.

[10] J. R. Morones, J. L. Elechiguerra, A. Camacho, K. Holt, J. B. Kouri, J. T. Ramirez and M. J. Yacaman, *Nanotechnology*, 2005, **16**, 2346-2353.
[11] R. Xiong, C. H. Lu, Y. R. Wang, Z. H. Zhou and X. X. Zhang, *J. Mater. Chem. A*, 2013, **1**, 14910-14918.
[12] I. Sondi and B. Salopek-Sondi, *J. Colloid Inter. Sci.*, 2004, **275**, 177-182.
[13] T. M. Benn and P. Westerhoff, *Environ. Sci. & Tech.*, 2008, **42**, 4133-4139.
[14] M. Nocchetti, A. Donnadio, V. Ambrogi, P. Andreani, M. Bastianini, D. Pietrella and L. Latterini, *J. Mater. Chem. B*, 2013, **1**, 2383-2393.
[15] H. Y. Lee, H. K. Park, Y. M. Lee, K. Kim and S. B. Park, *Chem. Commun.*, 2007, **28**, 2959-2961.
[16] K. Chaloupka, Y. Malam and A. M. Seifalian, *Trends Biotechnol*. 2010, **28**, 580-588.
[17] Q. L. Feng, J. Wu, G. Q. Chen, F. Z. Cui, T. N. Kim and J. O. Kim, *J. Biomed. Mater. Res.*, 2000, **52**, 662-668.
[18] Y. Matsumura, K. Yoshikata, S. Kunisaki and T. Tsuchido, *Appl. Environ. Microbiol.*, 2003, **69**, 4278-4281.
[19] Z. M. Xiu, Q. B. Zhang, H. L. Puppala, V. L. Colvin, P. J. J. Alvarez, *Nano Lett.*, 2012, **12**, 4271-4275.
[20] R. Ma, C. Levard, S. M. Marinakos, Y. Cheng, J. Liu, F. M. Michel, G. E. Brown and G. V. Lowry, *Environ. Sci. Technol.*, 2012, **46**, 752-759.
[21] G. X. Gu, J. X. Xu, Y. F. Wu, M. Chen and L. M. Wu, *J. Colloid Inter. Sci.*, 2011, **359**, 327-333.
[22] Z. W. Deng, H. B. Zhu, B. Peng, H. Chen, Y. F. Sun, X. D. Gang, P. J. Jin and J. L. Wang, *ACS Appl. Mater. Interfaces*, 2012, **4**, 5625-5632.
[23] B. Chudasama, A. K. Vala, N. Andhariya, R. V. Upadhyay and R. V. Mehta, *Nano Res*, 2009, **2**, 955-965.
[24] S. Poyraz, I. Cerkez, T.S. Huang, Z. Liu, L. T. Kang, J. J. Luo and X. Y. Zhang, *ACS Appl. Mater. Interfaces*, 2014, **26**, 20025-20034.
[25] P. C. Ma, B. Z. Tang and J. K. Kim, *Carbon*, 2008, **46**, 1497-1505.
[26] K. Y. Chun, Y. Oh, J. Rho, J. H. Ahn, Y. J. Kim, H. R. Choi and S. Baik, *Nat. Nanotechnol.*, 2010, **5**, 853-857.
[27] R. Pasricha, S. Gupta and A. K. Srivastava, *Small*, 2009, **5**, 2253-2259.
[28] C. P. Chen, P. Gunawan, X. W. Lou and R. Xu, *Adv. Funct. Mater.*, 2012, **22**, 780-787.
[29] M. Liong, B. France, K. A. Bradley and J. I. Zink, *Adv. Mater.*, 2009, **21**, 1684-1689.
[30] J. Z. Ma, J. T. Zhang, Z. G. Xiong, Y. Yong and X. S. Zhao, *J. Mater. Chem.*, 2011, **21**, 3350-3352.
[31] A. Gupat, M. Maynes and S. Silver, *Appl. Environ. Microbiol.*, 1998, **64**, 5042-5045.
[32] X. Wang, Y. Dai, J. L. Zou, L. Y. Meng, S. Ishikawa, S. Li, M. Abuobeidah and H. G. Fu, *RSC Adv.*, 2013, **3**, 11751-11758.
[33] M. M. Khin, A. S. Nair, V. J. Babu, R. Murugan and S. Ramakrishna, *Energy Environ. Sci.*, 2012, **5**, 8075-8109.

[34] A. Pratsinis, P. Hervella, J. C. Leroux, S. E. Pratsinis and G. A. Sotiriou, *Small*, 2013, **9**, 2576-2584.
[35] X. L. Zhang, H. Y. Niu, J. P. Yan and Y. Q. Cai, *Colloids Surf., A*, 2011, **375**, 186-192.
[36] S. Mukherjee, D. Chowdhury, R. Kotcherlakota, S. Patra, Vinothkumar B, M. P. Bhadra, B. Sreedhar, C. R. Patra, *Theranostics*, 2014, **4**, 316-335.
[37] Y. Cong, T. Xia, M. Zou, Z. N. Li, B. Peng, D. Z. Guo and Z. W. Deng, *J. Mater. Chem. B*, 2014, **2**, 3450-3461.
[38] P. Dalla, J. Tucek, D. Jancik, M. Kolar, A. Panacek and R. Zboril, *Adv. Funct. Mater.*, 2010, **20**, 2347-2354.
[39] H. Wang, J. Shen, G. X. Gao, Z. Gai, K. L. Hong, P. R. Debata, P. Banerjee and S. Q. Zhou, *J. Mater. Chem. B*, 2013, **1**, 6225-6234.
[40] H. H. Park, S. J. Park, G. P. Ko and K. Woo, *J. Mater. Chem. B*, 2013, **1**, 2701-2709.
[41] L. Zhang, Q. Luo, F. Zhang, D. M. Zhang, Y. S. Wang, Y. L. Sun, W. F. Dong, J. Q. Liu, Q. S. Huo and H. B. Sun, *J. Mater. Chem.*, 2012, **22**, 23741–23744.
[42] Y. J. Chen, N. Gao and J. Jiang, *Small*, 2013, **9**, 3242-3246.
[43] S. H. Xuan, Y. X. J. Wang, J. C. Yu and K. C.-F. Leung, *Chem. Mater.*, 2009, **21**, 5079–5087.
[44] K. S. Suslick, *Science*, 1990, **247**, 1439-1445.
[45] S. H. Xuan, Y.-X. J. Wang, J. C. Yu and K. C.-F. Leung, *Langmuir*, 2009, **25**, 11835-11843.
[46] H. P. Klug, L. E. Alexander, *X-ray Diffraction Procedures for Polycrystalline and Amorphous Materials; Wiley, New York*, 1962, pp.491-538.
[47] D. Lee, R. E. Cohen and M. F. Rubner, *Langmuir*, 2005, **21**, 9651-9659.
[48] S. Egger, R. P. Lehmann, M. J. Height, M. J. Loessner and M. Schuppler, *Appl. Environ. Microbiol.*, 2009, **75**, 2973–2976.
[49] P. Gong, H. Li, X. He, K. Wang, J. Hu, W. Tan, S. Zhang and X. Yang, *Nanotechnology*, 2007, **18**, 285604.
[50] N. Nino-Martinez, G. A. Martinez-Castanon, A. Aragon-Pina, F. Martinez-Gutierrez, J. R. Martinez-Mendoza and F. Ruiz, *Nanotechnology*, 2008, **19**, 065711.
[51] J. Njagi, M. M. Chernov, J. C. Leiter and S. Andreescu, *Anal. Chem.*, 2010, **82**, 989-996.
[52] I. F. Tannock, D. Rotin, *Cancer Research*, 1989; **49**: 4373-84.